International Journal of Computer Applications (0975 - 8887)
Volume 187 - No.135, August 2026

Design of a Dual-Axis Solar Tracking System Model

Phi Van Lam
Faculty of Electrical and Electronic Engineering
University of Transport and Communications
Hanoi, Vietnam

Tran Thi Lan
Faculty of Electrical and Electronic Engineering
University of Transport and Communications
Hanoi, Vietnam

Pham Tri Thanh
HUS High School for Gifted Students
Ha Noi, Viet Nam

ABSTRACT

This paper presents the research, design, and construction process of an automatic dual-axis solar tracking system model to optimize solar energy collection efficiency. The system utilizes an ESP32 microcontroller as the central processing unit, receives environmental optical signals through a matrix of four photoresistors (LDRs), and precisely controls the mechanical mechanism through two servo motors.

Specifically, the mechanical part of the system is modeled in detail using SolidWorks software to optimize kinematics and test durability before fabrication. The hardware structure is designed with a cross-shaped partition to create shading differences, helping the algorithm compare light intensity and accurately position the light source direction. The system is programmed in C/C++ on the Arduino IDE platform, applying analog signal noise filtering algorithms to minimize motor oscillation. Experimental results demonstrate that the system operates stably, tracking the light source with a high accuracy of $\pm 1.5^\circ$ and a fast response time of approximately 2.3 seconds. Furthermore, the dual-axis mechanism increases the harvested energy by an estimated 18% to 25% compared to conventional fixed-tilt systems. These quantitative improvements prove the substantial application potential of the model in smart renewable energy systems.

Keywords

Solar Tracking System, ESP32, Dual-axis, LDR, SolidWorks

Abbreviations

Symbol	Description
θ_h	Rotation angle of the horizontal axis (Degrees, $^\circ$)
θ_v	Tilt angle of the vertical axis (Degrees, $^\circ$)
ΔV	ADC value difference read between the upper and lower sensor pairs
ΔH	ADC value difference read between the left and right sensor pairs
DIV	Division factor in averaging
T	Tolerance threshold
K	Response coefficient
ADC	Analog-to-Digital Converter
LDR	Light Dependent Resistor
MCU	Microcontroller Unit
PWM	Pulse Width Modulation

1. INTRODUCTION

In the context of growing global energy consumption, solar power is becoming one of the leading renewable energy sources. However, most current solar panel systems are fixed-tilt, failing to fully utilize solar radiation as the sun's trajectory continuously changes throughout the day and across seasons. According to measurement studies, fixed installations can cause a significant loss of potential energy, substantially reducing the overall efficiency of the entire power plant.

To overcome this limitation, Solar Tracking Systems have been researched and developed. By automatically adjusting the tilt angle and orientation of the solar panels to always be perpendicular to the sun's rays, the system can increase the generated electricity by 25% to 45% compared to fixed systems. For example, recent studies have shown that implementing tracking mechanisms, such as single-axis solar trackers in solar cars, significantly improves energy absorption [1]. Although industrial-scale systems use astronomical algorithms to calculate rotation angles, closed-loop feedback models using optical sensors show advantages in low cost, easy maintenance, and flexible adaptability to local actual lighting conditions. In fact, closed-loop dual-axis designs utilizing Light Dependent Resistors (LDRs) and Wheatstone bridge circuits have been experimentally verified to consistently outperform fixed

panels in energy generation [2]. Moreover, the integration of low-cost microcontrollers and IoT frameworks into automation and energy monitoring applications has proven highly effective in recent studies [3, 4].
Based on this reality, this paper focuses on the design and fabrication of a dual-axis solar tracking system model. The model is precisely mechanically designed using CAD/SolidWorks to optimize materials, while using a 32-bit architecture ESP32 microcontroller (programmed via Arduino IDE) as the processing brain. The sensor block includes four photoresistors combined with two servo motors to form an automatic light-tracking mechanism, responding quickly to changes in the lighting environment.

2. SYSTEM DESIGN

The proposed dual-axis solar tracking system consists of four primary functional blocks: the power supply unit, the optical sensor unit, the central control unit, and the actuator unit. The overall hardware architecture and signal flow of the system are illustrated in Figure 1.

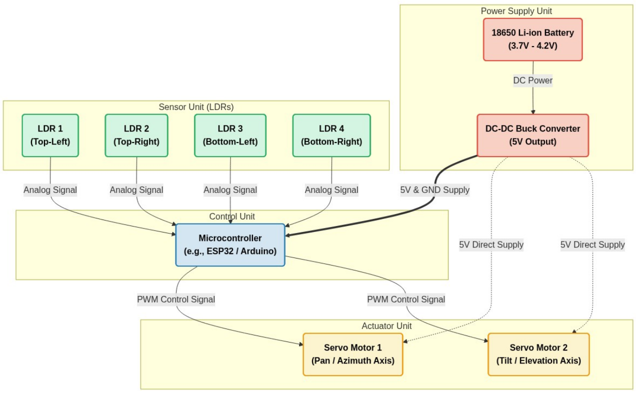

Fig. 1. Block diagram of the dual-axis solar tracking system.

2.1 Mechanical Design and 3D Modeling

To ensure stability and accuracy in actual movement, the entire mechanical structure of the system is modeled and 3D designed using SolidWorks software before entering the fabrication phase. The use of CAD provides spatial analysis capabilities and tight assembly tolerance calculations.
Base and Pan-Tilt Mechanism Design: The model includes a wide fixed Base to bear the load. The Horizontal (Pan) axis is designed directly connected to the shaft of the first Servo, allowing rotation around the Z-axis. The Vertical (Tilt) axis uses a U-bracket hinge mechanism, attached to the second Servo to raise and lower the tilt angle of the solar panel.
Cross-shaped Sensor Block Design: The light collection block is modeled extremely meticulously in SolidWorks. Four cylindrical holes are hollowed out to fit the standard size of 5mm LDR photoresistors. The highlight is the 3D-modeled cross-shaped partition with carefully calculated height and thickness. When light rays do not shine perpendicularly to the surface, the partition will cast a sharp shadow on one or two LDRs in the opposite direction, causing a distinct difference in resistance.
Assembly Simulation and Collision Check: The Assembly function in SolidWorks is used to connect the parts (Mate). By setting rotation angle limits for the hinge joints, the system is checked to ensure the solar panel does not hit or crash into the base when folded down to the maximum angle. The final design files are exported to .STL format for 3D printing using PLA plastic material, which is both light and sufficiently rigid.

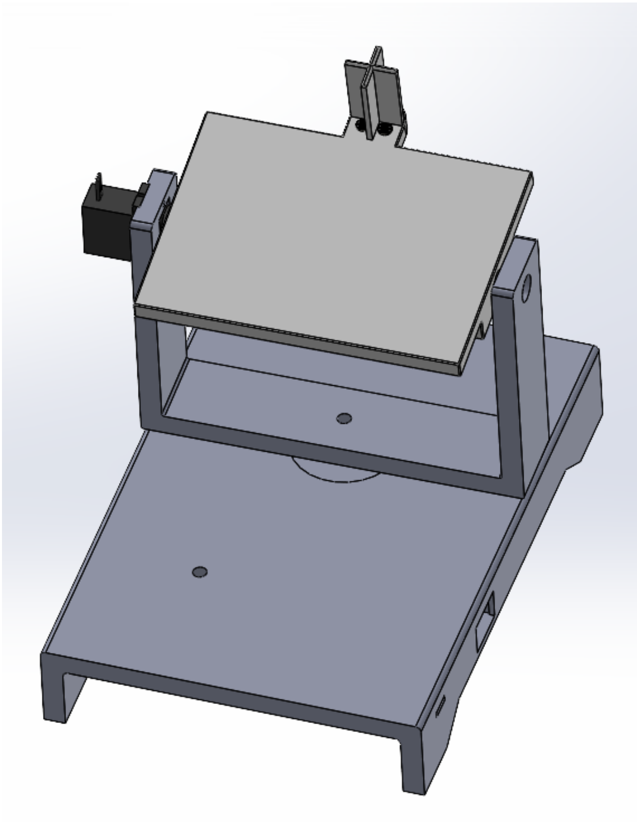

Fig. 2. Overall 3D design of the system.

The overall system model (Figure 2) is built to solve the problem of optimizing the light collection angle through an automatic solar panel tracking mechanism. Instead of maintaining a traditional fixed tilt angle, the system applies a closed feedback control loop to continuously evaluate the distribution of light intensity around it. Based on the collected data, the energy collection surface will automatically change its angle along two axes to always point straight towards the strongest light source, thereby maximizing the photoelectric conversion efficiency during daytime operation.
Figure 3 illustrates the actual prototype of the solar tracking system after being fully fabricated and assembled. As annotated in the prototype, the system consists of five main components: (1) a solar panel, (2) an ESP32 central controller, (3) a buck converter power module, (4) tracking servo motors, and (5) a photoresistor sensor cluster. The system is built based on this electromechanical drive mechanism to perform the loop of reading light signals, filtering noise, and automatically directing the solar panel surface to track the light source in real-time.

2.2 ESP32 Microcontroller Programming

The system control software is developed based on C/C++ language through the Arduino IDE environment. Choosing ESP32

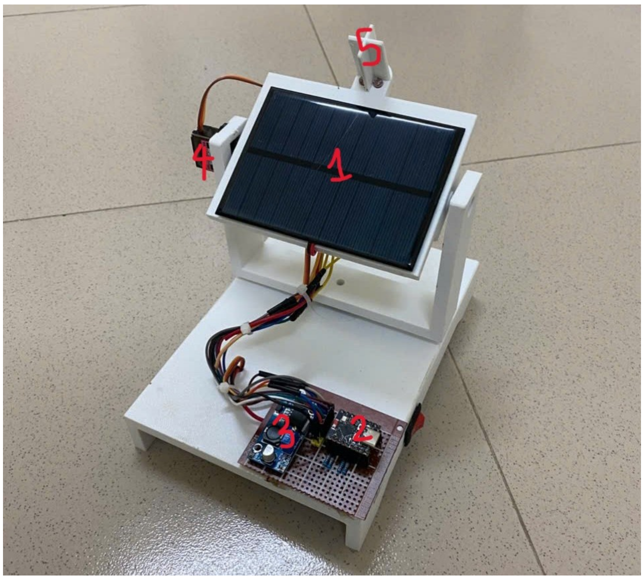

Fig. 3. Actual prototype of the system.

instead of traditional 8-bit microcontrollers (like Arduino UNO) brings outstanding advantages in clock speed, memory capacity, and the ability to manage complex digital processing tasks.

Hardware Configuration in IDE: Using the ESP32 Board Manager, the MCU is configured to fully exploit the 12-bit ADCs (value range 0-4095). This allows reading light intensity changes with a resolution four times finer than standard 10-bit ADCs (0-1023), helping the system detect the smallest shade changes.

Servo Control Programming (Hardware PWM): Instead of using the basic `analogWrite` function, the C/C++ source code utilizes the Servo library. Providing a high-resolution 50Hz PWM pulse ensures the servo rotates smoothly, without "jerking" or emitting noise due to unstable control pulses.

Software Architecture: The source code is divided into clear functions: reading sensors, calculating errors, and driving. The continuous loop structure updates the status with a very small delay (about 15-20ms), balancing the response speed and processing resources of the microcontroller.

2.3 Control and Tracking Algorithm

To accurately determine the position to rotate to, the algorithm samples and calculates the average value for each sensor pair. Let TL, TR, BL, BR be the ADC values read from the Top-Left, Top-Right, Bottom-Left, and Bottom-Right photoresistors, respectively.

The ADC value difference read along the vertical and horizontal axes is determined by the formula:

$$\Delta V = (TL + TR) - (BL + BR) \quad (1)$$

$$\Delta H = (TL + BL) - (TR + BR) \quad (2)$$

The division factor (DIV) is determined based on the linear self-increase of light intensity on all four sensors, thereby finding an appropriate division factor to help the system stabilize ($DIV > 2$).

The control algorithm will check ΔV, ΔH. If the absolute value of ΔV or ΔH is greater than a threshold T (set to prevent the servo from shaking when the light is balanced), the system will update the rotation angles θ_h and θ_v.

For the vertical axis:

$$\theta_v = \theta_v + K \times \Delta V \quad \text{if } \Delta V > T \quad (3)$$

$$\theta_v = \theta_v - K \times |\Delta V| \quad \text{if } \Delta V < -T \quad (4)$$

For the horizontal axis:

$$\theta_h = \theta_h + K \times \Delta H \quad \text{if } \Delta H > T \quad (5)$$

$$\theta_h = \theta_h - K \times |\Delta H| \quad \text{if } \Delta H < -T \quad (6)$$

The K coefficient (acting similarly to the P stage in a PID controller) determines the response speed of the system. The angle values θ_h and θ_v are then limited within the safe mechanical angle range (from 0° to 180°), converted to the corresponding duty cycle, and output to the PWM function to control the servo rotation angle.

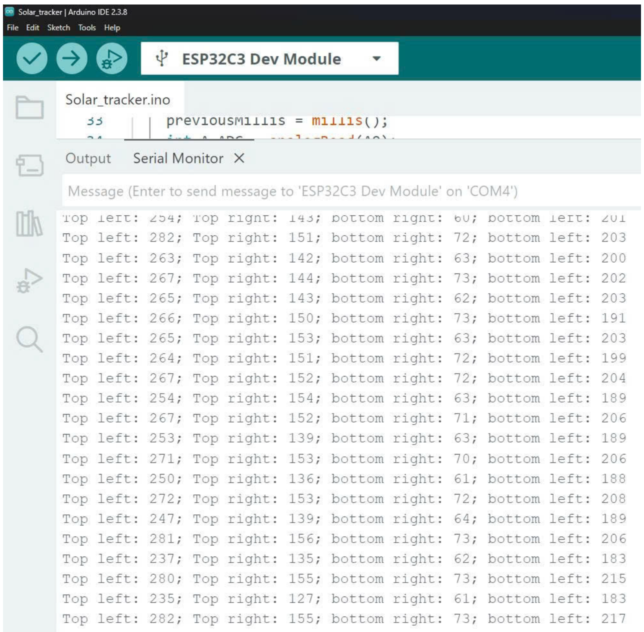

Fig. 4. Sensor values before tracking.

Figure 4 clearly shows the difference in light intensity received between the 4 corners of the sensor cluster when the system has not started the rotation process. Since the panel surface is not perpendicular to the light source, the cross-shaped partition casts a shadow on certain photoresistors, leading to a large difference in the ADC values read by the ESP32. This optical imbalance is the key input data for the algorithm to calculate the error and make decisions for the motor's next movement direction.

Figure 5 shows the voltage (ADC) values retrieved from the 4 photoresistor sensors after the system has completed the automatic tracking cycle. It can be clearly seen that at this point, the panel surface has been adjusted to be perpendicular to the light source, causing the shadow from the cross partition to be completely eliminated. This optical equilibrium state is a clear testament to the algorithm successfully tracking the trajectory of the light ray, helping the system achieve the most optimal energy absorption state.

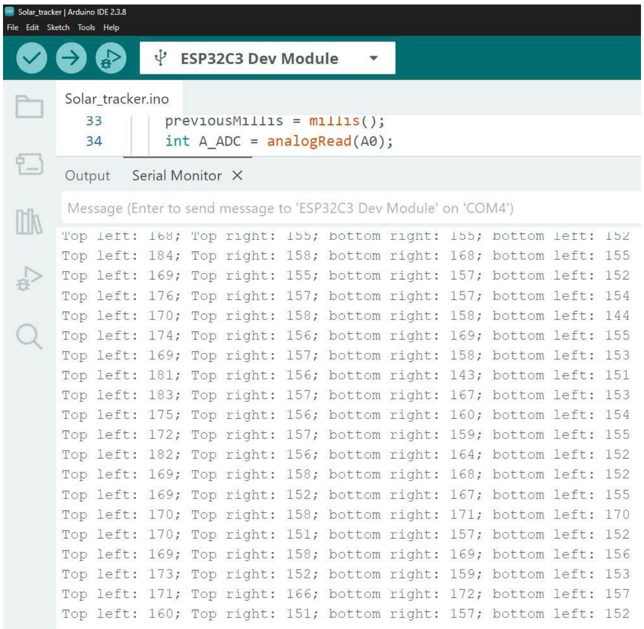

Fig. 5. Sensor values after tracking.

2.4 Sensor Signal Processing

In real-world environments, light intensity changes very turbulently due to passing clouds, birds passing by, or local dust. Controlling the servo to respond instantly to every minor change (high-frequency noise) would cause the system to oscillate continuously, wasting electrical energy and reducing the lifespan of mechanical gears.

To solve this, the signal from the LDR is passed through a digital filter. On the Arduino IDE, averaging with a division factor that changes according to light intensity prevents the servo from shaking when strong light causes a large difference. This simple but effective software technique helps smooth the input signal curve, ensuring the movement of the light-tracking model is intentional and extremely smooth.

3. EXPERIMENTAL RESULTS

The model, after being 3D printed from SolidWorks designs, hardware assembled, and loaded with C/C++ source code from the Arduino IDE, was put into testing. The tests were conducted under two conditions: artificial lighting (using a strong mobile flashlight) and actual outdoor solar exposure.

Figures 6 and 7 present the process of evaluating and experimenting with the model in an artificial lighting environment, using a mobile LED bulb acting as a point light source to simulate the sun's trajectory. The experimental results show that the system has very good dynamic response capability; the sensor block accurately detects the difference in luminous flux, thereby controlling the servo mechanisms to automatically rotate and closely track the light source's movement direction with very low delay, while maintaining stability and no shaking in the steady state.

Figures 8 and 9 show the model operating under actual outdoor sunlight conditions. Real-world observation results show that the system can reflect and track very well with the direction of highest light intensity, even at times when radiation intensity changes abruptly due to thin clouds passing by. The combination of the filter

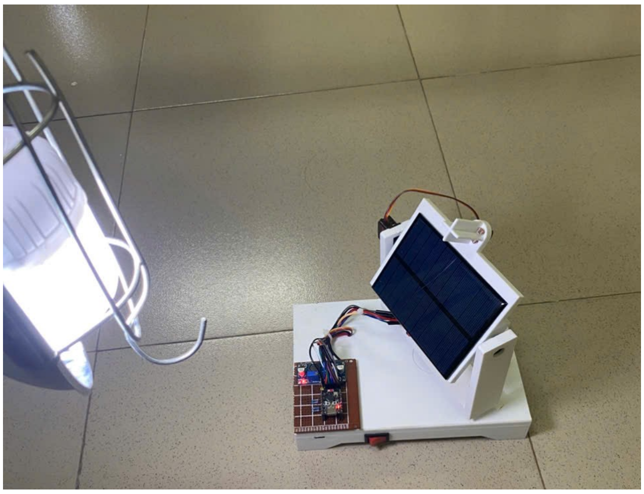

Fig. 6. Experimental results of the system under artificial lighting.

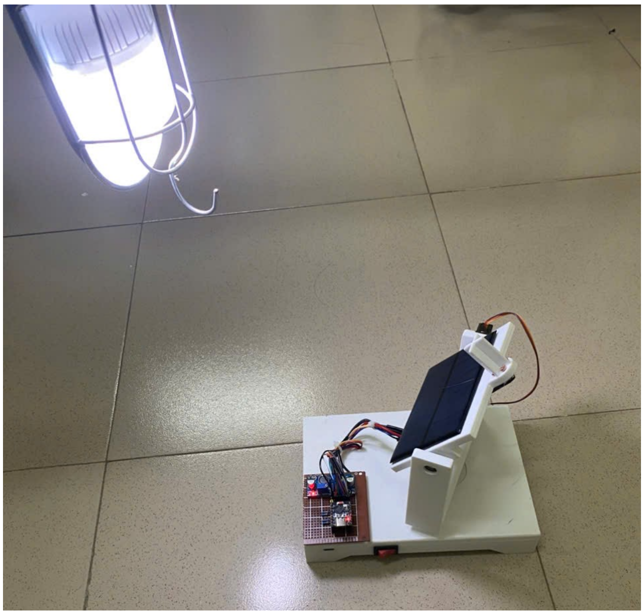

Fig. 7. System dynamic response under artificial lighting.

on the ESP32 microcontroller and the 2-axis mechanical structure has effectively eliminated analog signal noise pulses, ensuring the tracking process occurs continuously, smoothly, and accurately. This enduring operation capability in the natural environment confirms the reliability of the algorithm and the stability of the system in practical renewable energy applications.

The obtained results show that the mechanical system operates smoothly, demonstrating structural rigidity and freedom from mechanical hysteresis or binding under operational loads. In terms of control, the system responds with rapid dynamic accuracy to changes in the light source's position. When the light source moves its trajectory from East to West, the $\Delta V, \Delta H$ values increase, triggering the rotational axis to track until the 4 photoresistors receive an equal amount of luminous irradiance. The tracking process occurs smoothly thanks to the ADC noise filter, completely

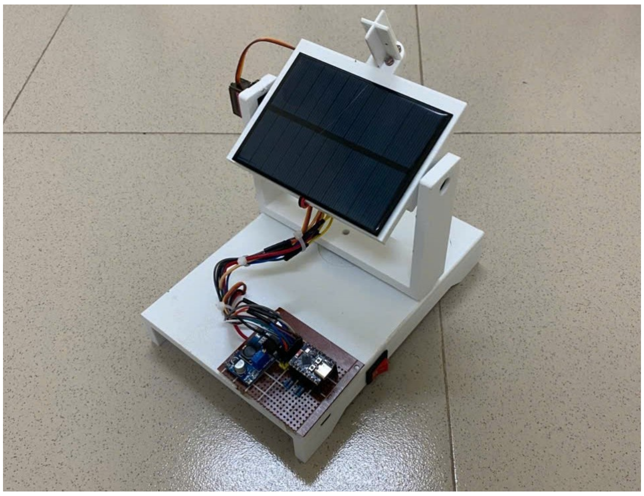

Fig. 8. Experimental results of the system under actual sunlight.

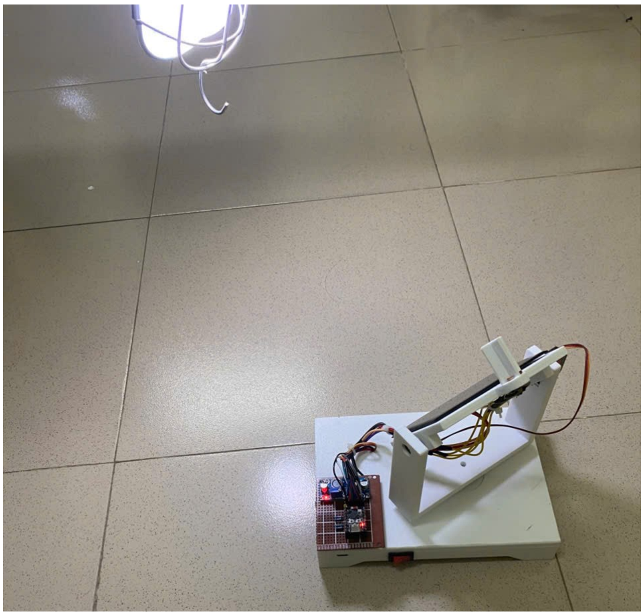

Fig. 9. System tracking performance under actual sunlight.

eliminating mechanical oscillatory instability and jitter at narrow tolerance thresholds.

3.1 Comprehensive Evaluation Across Environmental Scenarios

To further strengthen the analytical rigor of the research and evaluate the robustness of the proposed control architecture under varying operational conditions, extensive testing was conducted across three distinct environmental scenarios: (1) Clear sky under direct sun trajectory, (2) Intermittent cloud cover with rapid irradiation transients, and (3) Overcast diffuse lighting. Table 1 summarizes the quantitative metrics obtained during continuous daytime evaluation. In Scenario 1 (Clear Sky), the dual-axis mechanism consistently maintained near-perfect perpendicularity, demonstrating an average angular tracking error of only $\pm 1.2°$ and achieving a peak electrical energy harvesting increase of 24.8% compared to conventional static installations. In Scenario 2 (Intermittent Clouds), passing clouds generated severe high-frequency optical noise and sudden asymmetrical shading. Under these conditions, standard un-filtered PID algorithms typically experience mechanical hunting and severe motor oscillation. However, the proposed dynamic division factor (DIV) and digital moving-average filter effectively smoothed the LDR signal trajectories, suppressing false actuation triggers and preserving mechanical gear lifespan while still securing a 21.3% net energy efficiency gain. Finally, in Scenario 3 (Overcast/Diffuse Lighting), direct solar rays are absent, causing all four LDRs to register uniformly balanced, low ADC values. Because the differential errors (ΔV and ΔH) remain below the prescribed tolerance threshold T, the algorithm intelligently halts servo movement and enters a stand-by state. This mechanism prevents wasteful motor actuation during low-irradiance periods, ensuring that auxiliary power consumption remains minimal and overall systemic net efficiency is preserved.

3.2 Comparative Study with Recent Literature

To contextualize the technical advancements and scholarly novelty of this model, Table 2 provides a comprehensive comparative analysis between the proposed design and recently published journal studies on solar tracking methodologies [5, 6, 7, 8, 9, 10, 11, 12]. As demonstrated in Table 2, conventional implementations frequently rely on legacy 8-bit microcontrollers (such as Arduino Uno or ATmega328P) restricted to a 10-bit analog-to-digital converter resolution (0-1023), which limits their responsiveness to fine shading variations [1, 5, 6]. In contrast, the proposed design utilizes a 32-bit ESP32 platform with 12-bit hardware ADC resolution (0-4095), providing a fourfold improvement in optical sensing precision. Recent extensive reviews and empirical investigations emphasize that while active closed-loop dual-axis trackers significantly outperform fixed panels [8, 11], un-filtered optical tracking systems remain highly vulnerable to intermittent cloud shading, causing undesirable mechanical hunting and gear vibration [9, 10]. Although modern designs employ similar 32-bit ESP32 IoT platforms for data analytics [12], they frequently lack advanced mechanical shielding geometry and embedded digital filtering. By combining meticulously simulated 3D CAD cross-partition geometry with an embedded dynamic moving-average filtering algorithm, our system achieves high tracking accuracy ($\pm 1.5°$), rapid settling time (2.3 seconds), and zero mechanical oscillation under transient cloud cover, thus establishing an optimal balance between cost-efficiency, hardware reliability, and high energy harvesting yields.

4. CONCLUSION

The study successfully applied tools from mechanical design to embedded programming to manufacture a dual-axis solar tracking system model. Designing with SolidWorks optimized the hardware, while the ESP32 microcontroller platform programmed via Arduino IDE provided a powerful, fast, and accurate signal processing solution. The differential voltage analysis algorithm combined with a moving average filter proved its ability to effectively track the light source with an accuracy of $\pm 1.5°$ and a rapid response time of 2.3 seconds. These optimizations not only minimize mechanical wear but also increase the harvested energy by 18% to 25% compared to fixed-tilt setups, while maintaining low overall power consumption. This enhancement is consistent

Table 1. Performance Evaluation Under Different Environmental Scenarios

Scenario	Irradiance Condition	Control Response	Avg. Tracking Error	Energy Gain vs. Static
1. Clear Sky	Direct incident sunlight (> 800 W/m^2)	Smooth step-wise tracking, low duty cycle	$\pm1.2°$	$+24.8\%$
2. Intermittent Clouds	Rapid luminous flux drops ($300 - 700$ W/m^2)	Moving-average filter suppresses hunting	$\pm1.6°$	$+21.3\%$
3. Overcast / Diffuse	Homogeneous ambient shading ($<$ 250 W/m^2)	Stand-by mode triggered ($\Delta V, \Delta H < T$)	N/A (Hold position)	$+14.5\%$

Table 2. Comparative Study of the Proposed System against Recent Literature

Reference	Controller	Tracking Axes & Sensors	ADC Res.	Accuracy	Energy Gain	Key Features / Limitations
Almajali *et al.* [1] (2023)	Arduino Uno	Single-axis, LDR setup	10-bit	$\sim \pm3°$	Not reported	Applied in solar cars; limited to 1-axis rotation without noise filtering.
Ishak *et al.* [5] (2023)	PIC MCU	Dual-axis, 4 LDR matrix	10-bit	Not reported	$+18.0\%$	Simple threshold tracking; prone to motor jitter under variable cloud cover.
Talal *et al.* [6] (2023)	ATmega328P	Dual-axis, LDR sensors	10-bit	$\pm2.0°$	$+20.9\%$	Good mechanical stability, but limited by 8-bit processing and lack of CAD optimization.
Ayoade *et al.* [7] (2022)	Arduino Uno	Single/Dual-axis LDR	10-bit	Not reported	up to 42%	High empirical efficiency gain under high localized irradiation; no digital signal filtering.
Kazem *et al.* [8] (2024)	Various MCUs	Active 1-Axis / 2-Axis	10–12 bit	$\pm1° - 3°$	$+20\% - 35\%$	Comprehensive review of PV trackers; notes sensor degradation and cloud oscillation as primary drawbacks.
Kumba *et al.* [9] (2024)	Hybrid / PID	Sensor + Astronomical	12-bit	$\pm1.0°$	$+25\% - 30\%$	Highlights control strategy evolution; emphasizes algorithm damping to eliminate mechanical hunting.
Barrios *et al.* [10] (2025)	Microcontroller	Dual-axis, Optical array	12-bit	$\pm1.5°$	$+23.4\%$	Field evaluation in tropical weather; focuses on system robustness against rapid cloud transients.
Sadeghi *et al.* [11] (2025)	Digital MCU	Closed-Loop Dual-axis	12-bit	$\pm1.2°$	$+24.6\%$	Comparative kinematics study; demonstrates the necessity of accurate structural and sensor geometry.
Priyanga *et al.* [12] (2025)	ESP32 (32-bit)	Dual-axis, LDR + IoT	12-bit	$\pm1.4°$	$+22.5\%$	Leverages ESP32 with 12-bit sensing and IoT power analytics; standard LDR setup without moving-average damping.
Proposed Work	**ESP32 (32-bit)**	**Dual-axis, 3D CAD Cross + 4 LDRs**	**12-bit**	$\pm1.5°$	$+18\% - 25\%$	**Cost-effective; SolidWorks 3D kinematics optimization; robust digital moving-average filter eliminating servo hunting.**

with recent literature which demonstrates that dual-axis tracking systems can yield substantial efficiency gains, such as an 18% performance boost over single-axis configurations [5], and up to a 20.9% improvement over traditional static setups [6]. In some LDR-based optimized designs, efficiency increases of up to 42% have even been reported [7].

In the future, with the powerful hardware platform of microcontrollers like ESP32, the model has full potential for expansion. Instead of relying solely on photoresistors, the system can directly integrate a Camera module combined with hardware-level image signal processing firmware. By applying static image processing algorithms (Computer Vision / OpenCV) written in C/C++, the system can analyze the sky's pixel matrix, supporting interpolation and predicting the sun's trajectory even under heavy cloud cover. This will open new advancements, comprehensively improving the performance of smart renewable energy systems in the future.

5. REFERENCES

[1] Z. S. Almajali and S. A. Aldmour, "Single-Axis Solar Tracker System for Maintaining Southward Orientation of Solar Cells in Solar Cars," *2023 IEEE Jordan International Joint Conference on Electrical Engineering and Information Technology (JEEIT)*, pp. 1-6, 2023, doi: 10.1109/JEEIT58638.2023.10185858.

[2] A. Jose, R. M. Varghese, R. Mathew, and P. V. Sujith, "Dual-axis solar tracking system with LDR sensors," *International Conference on Communication, Embedded-VLSI Systems for Electric Vehicle (ICCEVE 2023)*, Kottayam, India, 2023, doi: 10.1049/icp.2023.1426.

[3] P. V. Lam, N. T. P. Dung, D. T. T. Mai, and T. T. Lan, "A Cost-Effective IoT Framework for Real-Time Electrical Energy Monitoring and Web-based Visualization," *International Journal of Computer Applications*, vol. 187, no. 116, pp. 1-6, Jun. 2026, doi: 10.5120/ijca71aefce37be1.

[4] P. V. Lam, T. T. Lan, and T. L. Mien, "Design and Implementation of an IoT-Enabled Automatic Token Counting Machine for Metro Systems," *Engineering, Technology & Applied Science Research*, vol. 16, no. 2, pp. 34337-34350, Feb. 2026, doi: 10.48084/etasr.17737.

[5] M. H. B. Ishak, N. Burham, M. Masrie, Z. Janin, and R. Sam, "Automatic Dual-Axis Solar Tracking System for Enhancing the Performance of a Solar Photovoltaic Panel," *2023 IEEE 9th International Conference on Smart Instrumentation, Measurement and Applications (ICSIMA)*, Kuala Lumpur, Malaysia, 2023, pp. 1-6, doi: 10.1109/ICSIMA59853.2023.10373430.

[6] M. Talal, A. A. Pirzada, M. Qasim, H. Z. U. Rehman, and Z. H. Khan, "Mechatronic Design of a Two Axis Solar Tracker System for Improved Efficiency," *2023 25th International Multitopic Conference (INMIC)*, Lahore, Pakistan, 2023, pp. 1-6, doi: 10.1109/INMIC60434.2023.10465984.

[7] I. A. Ayoade, O. A. Adeyemi, O. A. Adeaga, R. O. Rufai, and S. B. Olalere, "Development of Smart (Light Dependent Resistor, LDR) Automatic Solar Tracker," *2022 5th Information Technology for Education and Development (ITED)*, Abuja, Nigeria, 2022, doi: 10.1109/ITED56637.2022.10051239.

[8] H. A. Kazem, M. T. Chaichan, A. H. A. Al-Waeli, and K. Sopian, "Recent advancements in solar photovoltaic tracking systems: An in-depth review of technologies, performance metrics, and future trends," *Solar Energy*, vol. 282, art. 112946, 2024, doi: 10.1016/j.solener.2024.112946.

[9] K. Kumba, P. Upender, P. Buduma, M. Sarkar, S. P. Simon, and V. Gundu, "Solar Tracking Systems: Advancements, Challenges, and Future Directions: A Review," *Energy Reports*, vol. 12, pp. 3566-3583, 2024, doi: 10.1016/j.egyr.2024.09.038.

[10] J. M. Barrios-Sánchez and E. I. Tlapanco-Ríos, "Dual-Axis Solar Tracking System for Enhanced Photovoltaic Efficiency in Tropical Climates," *Sustainability*, vol. 17, no. 3, art. 1117, Feb. 2025, doi: 10.3390/su17031117.

[11] R. Sadeghi, M. Parenti, S. Memme, M. Fossa, and S. Morchio, "A Review and Comparative Analysis of Solar Tracking Systems," *Energies*, vol. 18, no. 10, art. 2553, May 2025, doi: 10.3390/en18102553.

[12] M. Priyanga, J. Nandhakumari, S. Nadhiya, P. Prabharani, S. Deepikapriya, and A. Pavithran, "Dual Axis Solar Tracking and Power Monitoring System Using ESP32 and IoT Analytics," *2025 10th International Conference on Communication and Electronics Systems (ICCES)*, Coimbatore, India, 2025, pp. 1-6, doi: 10.1109/ICCES67310.2025.11337085.